physica status solidi pss a
www.pss-a.com

Check for updates

Fundamental Aspects Concerning the Validity of the Standard Equivalent Circuit for Large-Area Silicon Solar Cells

Jan-Martin Wagner, Jürgen Carstensen, and Rainer Adelung*

The standard equivalent circuit of a solar cell amounts to a lumped description by separate diode and resistor elements. As its application to a large-area silicon solar cell effectively implies averaging the emitter resistance which, however, is closely coupled to the p–n junction, it is not self-evident that it works more or less well. Using an analytically solvable distributed series resistance model and systematically treating the deviations from the ideal case of zero emitter resistance, the equivalent circuit is found in linear order in the sheet resistivity. In this linear order, the lumped voltage losses are fully compatible with the integrated Joule losses; this compatibility turns out to be a necessary and sufficient condition for modeling the local series resistance of a large-area silicon solar cell. In higher orders of the sheet resistivity, however, the lumped voltage losses are not compatible with the integrated Joule losses, which means that the equivalent circuit cannot describe these higher orders. The equivalent circuit resulting from the linear-order lumped series resistance accounts for the experimentally observed variation of the lumped series resistance along the current–voltage characteristic, which turns out to be fully described by a dependence on the dark diode current only.

1. Introduction

The standard equivalent circuit of a solar cell, either as one- (cf. **Figure 1**a) or as two-diode model, is a very widespread model for the lumped description of the *I*–*U* (current–voltage) curve of all kinds of solar cells; it can be found in practically all textbooks, and it serves as a starting point for the introduction of commonly used solar cell parameters, such as the dark saturation current density, J_0, or the lumped series resistance, R_s. Usually, for a large-area silicon solar cell, these parameter values are taken as effective averages of the local properties. Note that this involves implicit expectations—namely, that local solar cell parameters can be measured sequentially as maps or simultaneously as images, and that certain averages of the maps/images (not necessarily the arithmetic mean value) equal the respective lumped values that correspond to the standard equivalent circuit. Yet, as long as it is not explicitly shown by theory that these expectations are fulfilled, it remains unclear whether this effective averaging is valid. To the best of our knowledge, a thorough derivation showing the validity of the standard equivalent circuit for large-area silicon solar cells and providing the relevant averaging relations is missing in the literature.

In general, a meaningful lumped description of a large-area silicon solar cell requires the translation of spatially resolved *I*–*U* curve parameters, given, e.g., as maps/images of such parameters, into lumped *I*–*U* curve parameter values by averaging. However, it is not self-understanding that this works because, due to the laterally distributed series-resistance network being closely coupled to the p–n junction and the nonlinear diode characteristics, some fundamental restrictions exist for relating the spatially varying properties to a meaningful lumped value by averaging local solar cell parameters. Yet, several approaches have been published for analyzing spatially resolved *I*–*U* curve parameters to estimate the contribution of each point of a solar cell to the lumped *I*–*U* curve and to derive maps/images of efficiency-related parameters: Some approaches focus on the series resistance,[1–16] some consider the dark saturation current,[4,8–10,13–20] some aim at the shunt strength,[21–26] some derive the efficiency,[13,14,27–30] and some consider the photocurrent[15,31–33] or the photocurrent collection efficiency.[34–36] As within their respective limits these approaches work well, the fundamental question arises why this is the case. In other words: Why does the standard equivalent circuit of a solar cell [cf. Figure 1a] may work at all as a replacement for the distributed network of resistances and p–n junctions of a solar cell [cf. Figure 1b]? Put differently: Under which circumstances is the lumped series resistance, completely decoupled from the p–n junction, a physically sensible parameter for a large-area solar cell?

Dr. J.-M. Wagner, Dr. J. Carstensen, Prof. R. Adelung
Institute for Materials Science
Technical Faculty
University of Kiel
Kaiserstr. 2, 24143 Kiel, Germany
E-mail: jwa@tf.uni-kiel.de

The ORCID identification number(s) for the author(s) of this article can be found under https://doi.org/10.1002/pssa.201900612.

© 2019 The Authors. Published by WILEY-VCH Verlag GmbH & Co. KGaA, Weinheim. This is an open access article under the terms of the Creative Commons Attribution License, which permits use, distribution and reproduction in any medium, provided the original work is properly cited.

DOI: 10.1002/pssa.201900612

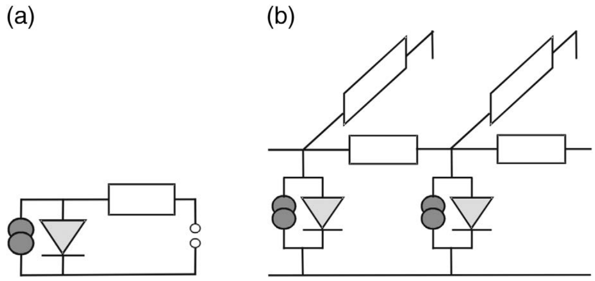

Figure 1. a) Standard equivalent circuit of a solar cell (here as one-diode model neglecting shunts), consisting of photocurrent source (medium gray), ideal diode (light gray), and series resistance (white). b) Section of a simplified distributed model for a solar cell, consisting of local solar cells connected in parallel by a series-resistance network [circuit symbols as in (a)]; two elementary units (to be laterally repeated) are shown.

Moreover, there are indications from experiment that an even deeper examination of the validity of the standard equivalent circuit for large-area silicon solar cells is needed: Several works in the literature show that the series resistance of large-area silicon solar cells is not constant but varies with the operating conditions (cf., e.g., refs. [37–41]), whereas the standard equivalent circuit lacks this effect as it contains a standard ohmic resistor having a constant value. We found that this variation is only related to the dark diode forward current, and that this behavior can empirically be described by a slightly modified equivalent circuit.[42] The question arises as to how one can understand this modified equivalent circuit from a theoretical point of view. To clarify this question is one of the purposes of the present fully theoretical work.

There are already some theoretical studies concerning the variation of the lumped series resistance of large-area silicon solar cells along the current–voltage characteristic.[43–48] However, they cannot explain the straightforwardness of our experimental results,[42] because their analytical expressions are much too complicated, or they miss the sole dependence on the dark diode forward current, or their results are given just numerically. In contrast, there are two theoretical works that explicitly state the conditions under which an equivalent lumped description of the distributed series resistance is possible, but only for a 1D geometry[49,50] which, as we discuss in Section 8, misses essential features of actual solar cells. In addition, although they help to understand the validity of the equivalent circuit in general, also the latter works lack the variation of R_s along the current–voltage characteristic, as a constant resistance value is obtained there. Here, we will show how to obtain both, the equivalent lumped description of the 2D-distributed series resistance and its variation along the current–voltage characteristic, from a consistent theoretical approach.

In this contribution, we analyze in detail under which condition(s) the lumped description by the standard equivalent circuit is, from a physical point of view, correct (yet, we do not claim to find all cases for which the standard equivalent circuit holds). This amounts to investigate the fundamental possibility to relate lumped (i.e., spatially averaged) and local (i.e., spatially resolved) I–U curves of such solar cells. As this involves the distributed series resistance, we will also investigate the theoretical description of local series resistances in detail. We will propose a fundamental condition—that it is necessary and sufficient to take into account distributed series-resistance effects in linear order in the sheet resistivity—which ensures that the standard equivalent circuit is applicable for describing the lumped I–U curve of large-area silicon solar cells. Moreover, when this fundamental condition holds, nearly all implicit expectations about the properties of local parameters are fulfilled. As a consequence of this fundamental condition, we will show how the distributed series resistance of a large-area silicon solar cell has to be taken into

Jan-Martin Wagner studied physics at the TU Berlin, with a diploma in theoretical solid-state physics. In 2004, he received his Ph.D. at the Institute of Condensed Matter Theory and Optics of the Friedrich-Schiller-Universität Jena for ab initio phonon calculations of strained GaN and AlN. In 2007, he changed to solar cell research, first in the group of Prof. Ulrich Gösele at the Max Planck Institute of Microstructure Physics in Halle (Saale), Germany, and from 2010 on in the group of Prof. Föll, CAU Kiel. He focuses on experimental and theoretical aspects of the series resistance.

Jürgen Carstensen began his studies in physics at the Christian-Albrechts-University of Kiel 1984 and received his Ph.D. from the Institute of Theoretical Physics in 1993 for work on superconductivity. Subsequently, he joined the materials science group of Prof. Helmut Föll at the Christian-Albrechts-Universität Kiel as a research associate. He began his work using semiconductor electrochemistry for the mapping of minority carrier life-time in solar-cell substrates and in the emerging field of porous semiconductors and related self-organization phenomena. He was instrumental in developing the unique spatially resolved "CELLO" solar-cell measurement technique.

Rainer Adelung studied physics at Kiel University, and after his doctoral degree in 2000, he changed to materials science in 2001 at the Case Western Reserve University, Ohio, USA. After his habilitation in 2007, he received a Heisenberg Professorship at Kiel University. From 2010 on, he holds the chair for functional nanomaterials; his research projects deal with porous and functional semiconductor materials. From 2013 to 2019, he was a spokesperson of KiNSIS, which is one of the priority research areas of Kiel University, and is currently managing director of the Institute for Materials Science.

© 2019 The Authors. Published by WILEY-VCH Verlag GmbH & Co. KGaA, Weinheim

account in the framework of the standard equivalent circuit; basically, we arrive at the same equivalent circuit as in our experiments.[42]

This article is organized as follows: In Section 2, we discuss in detail the fundamental difficulty related to series-resistance averaging and how this topic is related to the validity of the standard equivalent circuit. As a starting point for our further analysis, in Section 3, we discuss the reference case of zero emitter series resistance for which an equivalent circuit is trivially obtained just by averaging all currents. In Section 4, we introduce an analytically solvable 2D solar cell model which, after being treated in linear response, facilitates to discuss the physics behind the aspects relevant for the validity of the equivalent circuit, namely the properties of the lumped (Section 5) and the local (Section 6) series resistance. In Section 7, we show how the dark-current dependence of the distributed series resistance manifests itself in this model, and in Section 8, we generalize the analytical findings with regard to inhomogeneous solar cell properties, which facilitates to qualitatively explain some "standard" series-resistance properties of large-area solar cells; among other things, we motivate why taking the arithmetic average of local series resistances almost always gives a reasonable result. Finally, in Section 9, we arrive at a modified equivalent circuit of a silicon solar cell, and we show how the fundamental series-resistance averaging difficulty presented in Section 2 is avoided given that the newly proposed fundamental condition is met. Additionally, in the Analytical Section in the Supporting Information, we provide the mathematical details of our local series-resistance model, and we present a systematic treatment of the Joule losses and the voltage distribution in different orders of the sheet resistivity as a basis for the definition of a lumped series resistance. By explicitly showing the discrepancy between the series resistances obtained from the Joule losses and from the voltage distribution occurring already in second order of the sheet resistivity, we justify our newly proposed fundamental condition for the validity of the (modified) equivalent circuit.

Some parts of this work have previously been published as conference contributions; here they are linked and augmented by considering further aspects and by providing a deeper discussion to give a consistent view on the topic of the distributed series resistance of large-area silicon solar cells and the variation of its lumped value along the I–U curve.

2. Series Resistance Averaging

In general, a current I flowing through a standard ohmic resistor R has two consequences: It causes a certain voltage drop $U = RI$ and a certain Joule power loss $P = RI^2$ at this stand-alone two-terminal device. Therefore, from knowing the total current I and either the voltage drop U or the Joule power P, one can determine the relevant resistance. The top contact of a standard (H-type grid) large-area silicon solar cell, however, is a lateral network of different materials, and the current paths through this network may vary for different operating conditions of the solar cell; therefore, there is no straightforward definition of whatever kind of resistance for this network as such—and, therefore, also not for the solar cell as a whole. Nonetheless, in the literature, a large variety of series-resistance determination methods can be found (cf., e.g., refs. [51–55] for review works), each effectively establishing its own series-resistance definition.

As just discussed, there are two general ways to obtain a lumped R_s for a large-area solar cell: via a voltage drop or from the Joule power loss. Note, however, that there is a fundamental physical difference between these two: While power is an extensive quantity which is additive and therefore can be averaged, voltage is an intensive quantity which is not additive and therefore cannot be averaged; details are given below. So, only for the Joule power losses, the relevant theoretical concept to obtain a lumped R_s for a large-area solar cell is directly clear. For simplicity, here only the contribution of the emitter is considered: Integrating the local Joule heating power density $p = jE$ which, for the lateral sheet current density j_{lat} resulting from the external current flow, can be written as $p = \rho_{sh} j_{lat}^2$, gives the power loss P that, divided by the square of the total external current I_{ext}, yields the "Joule power loss series resistance" $R_P = P/I_{ext}^2$. This concept is otherwise model-free; especially, it does not involve the equivalent circuit. Therefore, it is suited to test the validity of the latter.

In contrast, the voltage-drop-based approach to obtain a lumped R_s is not that straightforward at all, because it is physically not sensible to average local solar cell voltages. This is so because "arithmetic averaging" means "to add up and to divide the result by the number of terms of the sum." But what does it mean to add up voltages? This can only be done when they are connected in series—which is not the case for the local solar cell voltages. Thus, taking an arithmetic average of local voltages is nonsense. Yet, the equivalent circuit effectively introduces an average voltage—namely one that describes the (mainly exponential) variation of the total dark current according to the behavior of one or two ideal p–n diode(s) plus, possibly, an ohmic shunt resistance. Disregarding the fundamental physical impossibility of voltage averaging, it is a standard approach in the literature (see the aforementioned reviews[51–55]) to obtain a "voltage drop series resistance" value R_U by means of applying the equivalent circuit. This means that, in contrast to R_P, R_U is not based on a fundamental physical concept but is restricted to the validity of the "effective voltage averaging" inherent in the equivalent circuit model. However, as mentioned in the Introduction, in the literature, there is no rigorous proof of the latter. Therefore, all equivalent-circuit-based "R_U recipes" have to be used with caution.

Before analyzing this "effective voltage averaging" in detail, we want to stress two important general aspects: First, we notice that for a truly ohmic behavior of a solar cell, there should be no difference between R_P and R_U, as the voltage drop and the Joule power loss caused by one and the same current flowing through a certain resistor are consistent with each other. However, as R_U is significantly less well defined compared with R_P, for large-area silicon solar cells, this will not hold in general. Instead, it is just an implicit expectation that all ohmic losses within a solar cell, considered as Joule heating, can be calculated just from the total external current I_{ext} and the "voltage drop series resistance" value R_U as total power $P = R_U I_{ext}^2$, giving the same value as from the lateral integration of p, leading to R_P.

Behind that expectation is the general question about the compatibility of these different ways of determining the series resistance. This question was refined and scrutinized in a numerical study by Micard and Hahn[56]; in a 2D simulation for a standard

 © 2019 The Authors. Published by WILEY-VCH Verlag GmbH & Co. KGaA, Weinheim

H-type grid silicon solar cell at maximum power point, they found that the sum of all local emitter Joule heating losses indeed equals the lumped value $R_{\mathrm{U}} I_{\mathrm{ext}}^2$. We will show that for solar cells for which the standard equivalent circuit as shown in Figure 1a is a physically sensible representation, ohmic losses can indeed be added up, but that it is not true in general for a distributed network schematically shown in Figure 1b; therefore, the question treated by Micard and Hahn is a fundamental one for the understanding of large-area silicon solar cells. Recently, this question was treated analytically for a 1D geometry by van der Heide and Poortmans[57]; they found that R_{P} and R_{U} give identical values only for sufficiently low lateral voltage variations.

The second aspect we want to stress is this: From the aforementioned two ways to obtain a resistance value and from the general properties of extensive and intensive quantities, it follows that the series resistance itself cannot be averaged because it is not extensive and therefore not additive; note, by the way, that it is not intensive either. Clearly, this is in contrast to the headline of the present Section ("Series Resistance Averaging"). Nonetheless, in the remainder of this Section, we will explicitly demonstrate the fundamental difficulty occurring when one still tries to average series resistances[58]; later on, we will even present a way to find a physically meaningful series-resistance average (see Section 6 and 9).

In the following, we consider—without loss of generality—the equivalent circuit in the one-diode model and analyze its "effective voltage averaging" in detail; as the local voltage on a large-area silicon solar cell is closely related to the local series resistance [cf. Equation (3)], this is basically the same as "series resistance averaging". In this model, the total external current–voltage characteristic, neglecting shunts, can be written as

$$\begin{aligned} I_{\mathrm{ext}} &= I_{01}\left[\exp\left(\frac{U_{\mathrm{ext}} - R_{\mathrm{s}} I_{\mathrm{ext}}}{U_{\mathrm{th}}}\right) - 1\right] - I_{\mathrm{ph}} \\ &=: I_{\mathrm{D}}(U_{\mathrm{ext}} - R_{\mathrm{s}} I_{\mathrm{ext}}) - I_{\mathrm{ph}} \end{aligned} \tag{1}$$

(Shockley equation including series resistance and photocurrent; $U_{\mathrm{th}} = kT/e$: thermal voltage). For each position (x, y) on the solar cell, where the individual "positions" are small areas given by the pixels of the scanning/imaging technique used in a measurement, one has basically the same equation, but here for the net local junction current (in vertical direction)

$$\begin{aligned} I_z(x,y) &= I_{\mathrm{D}}(x,y) - I_{\mathrm{ph}}(x,y) \\ &= I_{01}(x,y)\left[\exp\left(\frac{U(x,y)}{U_{\mathrm{th}}}\right) - 1\right] - I_{\mathrm{ph}}(x,y) \end{aligned} \tag{2}$$

where $U(x,y)$ is the local voltage; it incorporates the local series resistance. It is still an open issue—which we will address later—how to implement local series resistances, as there are two fundamentally different concepts: either together with the local junction current (cf. refs. [1,4,59] and later used in many works)

$$U(x,y) = U_{\mathrm{ext}} - R_{\mathrm{s}}(x,y) I_z(x,y) \tag{3a}$$

or with the total external current (cf. refs. [11,42,60])

$$U(x,y) = U_{\mathrm{ext}} - R_{\mathrm{s}}(x,y) I_{\mathrm{ext}} \tag{3b}$$

In the former case, typically the current density and an area-related series resistance are used. However, for systematic reasons, we prefer to use currents, as only currents explicitly add up (according to Kirchhoff's laws). Either way, the standard implicit assumption is that the lumped I–U characteristic, Equation (1), can be written as

$$\begin{aligned} I_{\mathrm{ext}} = \sum_{(x,y)} I_z(x,y) &= \left(\sum_{(x,y)} I_{01}(x,y)\right)\left[\exp\left(\frac{U_{\mathrm{ext}} - R_{\mathrm{s}} I_{\mathrm{ext}}}{U_{\mathrm{th}}}\right) - 1\right] \\ &\quad - \left(\sum_{(x,y)} I_{\mathrm{ph}}(x,y)\right) \end{aligned} \tag{4}$$

i.e., all lumped currents of Equation (1) have been replaced by the sums of the local currents, which is allowed because currents add up. Here, this can be done straightforwardly at short-circuit condition only, for which Equation (4) must hold as well. However, summing up Equation (2) and comparing with Equation (4) leads—for either version of the local voltage, Equation (3a) or (3b), therefore a dummy symbol $I_{\P}$ appears on the left-hand side of Equation (5), referring to either $I_z(x,y)$ or I_{ext}, accordingly—to the contradiction that

$$\sum_{(x,y)} I_{01}(x,y)\,\exp\left(-\frac{R_{\mathrm{s}}(x,y) I_{\P}}{U_{\mathrm{th}}}\right) \neq \left(\sum_{(x,y)} I_{01}(x,y)\right)\exp\left(-\frac{R_{\mathrm{s}} I_{\mathrm{ext}}}{U_{\mathrm{th}}}\right) \tag{5}$$

as the nonlinearity of the exponential function and the distributed series resistance network in general prohibit to exchange the order of summing up and applying the exponential function.

The inequality in Equation (5) means that, in the general case, the lumped R_{s} of the standard equivalent circuit is not able to correctly describe the collective effect of the local series resistances. On the other hand, this theoretical finding is in contrast to the experimental fact that the "effective voltage averaging" works on certain real solar cells. This means that there are solar cells for which an equals sign in Equation (5) holds, namely for those that can be described by the standard equivalent circuit. We will come back to this point at the end of Section 9; for now, we will discuss the implications of this experimental finding, being the starting point for the series-resistance concept presented in this work.

Clearly, the "effective voltage averaging" inherent in the standard equivalent circuit can be reasonable only for rather small voltage variations across the emitter: As the p–n junction forward current changes exponentially with voltage, it would lead to noticeably different dark current flow if there were systematically different voltages in certain areas of the solar cell, resulting in different operating points for these areas. Then, it probably would not make much sense to use the standard equivalent circuit because the latter describes the whole solar cell at a single effective operating point. "Rather small voltage variations across the emitter" means that the emitter is nearly an equipotential surface, which is the better fulfilled, the smaller the emitter sheet resistivity is. As our present approach is based on this fact, we discuss this in detail the following Section.

© 2019 The Authors. Published by WILEY-VCH Verlag GmbH & Co. KGaA, Weinheim

3. The Case of Zero Emitter Sheet Resistivity

For a hypothetical perfect emitter and grid having zero series resistance, the situation is trivial: Arbitrary lateral balancing currents may flow, perfectly equilibrating the voltage on the whole cell. Then, the voltage measured at an arbitrarily placed reference electrode holds for the whole cell. As a consequence, all local measurements can be straightforwardly interpreted as all contrast in the obtained map/image is solely due to the local material properties. Also, no restrictions exist for averaging: As all local photocurrents and local dark currents simply add up, they can be averaged. Therefore, all common implicit expectations—that local solar cell parameters can be measured and mapped and that averages of local parameter maps represent the corresponding lumped values—are fulfilled for zero emitter series resistance; the equivalent circuit is trivially obtained from the average photocurrent and the average dark currents (i.e., p–n junction forward current and shunt current). However, these expectations do not hold in general if considering the laterally distributed series-resistance network.

In this work, we consider lateral series-resistance effects on solar cells as deviations from the perfect zero-resistance grid, which is permitted as the emitter resistivity of standard industrial large-area silicon solar cells is rather low so that, under standard operating conditions, lateral voltage differences are small compared with the thermal voltage. That this approach is indeed physically justified comes out as a fundamental result. To that end, we perform systematic expansions of the equations in terms of the sheet resistivity $\rho_{\rm sh}$; the details are given in the Analytical Section in the Supporting Information. We mention that the two basic ideas of this concept, to make use of the fact that, for standard industrial solar cells, lateral voltage variations are small, and to use a series expansion in the sheet resistivity, is by far not new; the former was already used by Boone and van Doren[49] for what they called "properly designed" solar cells, both the latter and the former by Nielsen.[50]

In the following, we analytically solve a 2D model for which the interpretation of lumped and local solar cell parameters as shown in Figure 1 holds as well; the details are given in the Analytical Section in the Supporting Information. It turns out that for considering distributed series resistances only up to linear order in the sheet resistivity, all implicit expectations are still fulfilled, i.e., mapping and averaging of local series resistances leads to consistent results for the lumped cell parameters. This is a quite fundamental and not trivial result, because (as we will also show) the general 2D solution does not fulfill the implicit expectations, and for a 1D network not even the linear order solution fulfills all implicit expectations.

Equation (3a) is known as the model of independent diodes (or model of terminal-connected diodes, or multi-diode model). The conceptual starting point for this model is given by laterally fully isolated small solar-cell fragments, their size typically being defined by the correspondence to the pixels of the scanning/imaging technique used. In this model, lateral coupling effects between these fragments cannot be correctly accounted for, and the series resistance relevant for lateral balancing currents is significantly overestimated, especially for currents running over short distances. Note that, only in this model it makes sense to plot an "open-circuit map" (providing a local $U_{\rm oc}$ value as if the whole solar cell behaved as this pixel) for a fully finished solar cell (cf., e.g., refs. [13,14]) or to consider the effect of locally increased series resistance as potentially beneficial by limiting current losses due to, e.g., bad diodes (cf. refs. [61,62]); however, such approaches contradict the fundamental property of a strong coupling present in a 2D network due to lateral balancing currents which lead to the emitter nearly being an equipotential surface.

In contrast, on a silicon solar cell, the local voltage not only depends on the local junction current but also can be determined by all currents, especially lateral ones. In fact, typically the local junction current (density) has only a minor influence on the absolute value of the local voltage, compared with the combined effect of all neighboring junction currents. This can be seen as follows: For the emitter sheet current density, Ohm's law, $\vec{j}_{\rm em}(x,y) = \rho_{\rm sh}^{-1}\vec{E}(x,y)$, and the 2D continuity equation (with div_2 denoting the 2D divergence and $\vec{J}$ representing the bulk current density in the base), $\mathrm{div}_2\vec{j}_{\rm em}(x,y) = -J_z(x,y,z=0)$, lead (for constant sheet resistivity $\rho_{\rm sh}$) to the well-known general differential equation for the local emitter voltage $U_{\rm em}$ on a silicon solar cell (with Δ_2 denoting the 2D Laplace operator)

$$\Delta_2 U_{\rm em}(x,y) = \rho_{\rm sh} J_z(x,y,z=0) \tag{6}$$

i.e., the local vertical bulk current density J_z at the junction determines the local Laplacian of the voltage, not the voltage itself, and this brings in the influence of the neighboring junction currents on the local voltage. Therefore, Equation (3a)—i.e., the model of independent diodes—is inadequate for the description of large-area silicon solar cells, at least for those with a low sheet resistivity (resulting in a strong lateral coupling). The usage of the model of independent diodes for large-area silicon solar cells leads to various artifacts, e.g., in local series-resistance maps, most prominently in RESI[4] images where they are known as "shunt paradox",[63] or in current density maps where they are termed "resistive blurring".[16]

Therefore, in this work Equation (3b) is used, whereby the lateral voltage drops are considered as proportional to the total external current. As this amounts to a linear-response description of series-resistance effects, we suggest to use the abbreviation "LR-$R_{\rm s}$" to denote the series resistance defined by Equation (3b). The validity of the LR-$R_{\rm s}$ approach can easily be checked experimentally; we have found it to hold even for several amps of external current.[42] This justifies to call the proportionality constant between local voltage and total external current "local series resistance." Details of the LR-$R_{\rm s}$ concept will be given subsequently (and in the Analytical Section in the Supporting Information).

4. Analytical 2D Solar Cell Model: Linear Response Description

The first step in our approach is the linearization of the exponential I–U characteristic. This is physically sensible, as for commercial monocrystalline silicon (mono-Si) solar cells, under standard operating conditions, the lateral voltage variation is smaller than the thermal voltage (cf., e.g., results of luminescence measurements[4,64,65] or findings from the Corescan method[6]); the

 © 2019 The Authors. Published by WILEY-VCH Verlag GmbH & Co. KGaA, Weinheim

applicability of our approach to multicrystalline cells is discussed subsequently (Section 8). Without loss of generality we demonstrate this step here for a shunt-free single-diode model. The intended linearization amounts to a series expansion of the lateral voltage around a reference value $\overline{U}_\mathrm{D}$ representing the solar cell's working point under consideration. This voltage is found by the condition that it, when inserted in the relevant Shockley equation, leads to the total dark current $\overline{I}_\mathrm{D}$ of this working point. The slope of the ideal I–U characteristic at this working point is referred to by a lumped, area-related effective diode conductivity as

$$K := \frac{1}{A}\frac{\mathrm{d}I_\mathrm{D}}{\mathrm{d}U}\bigg|_{\overline{U}_\mathrm{D}} = \frac{\mathrm{d}J_\mathrm{D}}{\mathrm{d}U}\bigg|_{\overline{U}_\mathrm{D}} \tag{7}$$

(A: area of the solar cell, I_D: ideal diode forward current). Later on (in Section 6), we will show how this K can be introduced without referring to an ideal I–U characteristic (which is important as the ideal characteristic differs from the directly measurable one by the series resistance), but for the time being we prefer to use Equation (7).

For the working point under consideration, given by the total dark current $\overline{I}_\mathrm{D}$, let the local voltage be $U(x,y)$. Now consider the special open-circuit situation leading to the same total dark current. Let the voltage distribution of this corresponding open-circuit situation be given by the function $\overline{U}(x,y)$. Next, to describe the actual voltage distribution of the working point under consideration, we consider the deviation $\widetilde{U}(x,y)$ from the reference distribution, i.e., we consider the local voltage broken up as $U(x,y) = \overline{U}(x,y) + \widetilde{U}(x,y)$. Here and in the following, we use a general notation principle: All quantities referring to the solar cell's open-circuit working point are indicated by an overline, all variational quantities by a tilde. As our basic approximation, we describe the resulting deviation in the local dark current density by

$$\widetilde{J}_\mathrm{D}(x,y) = K\widetilde{U}(x,y) \tag{8}$$

with the area-related diode conductivity K from Equation (7); originally, it was introduced as such in ref. [3]. The thereby-obtained analytical 2D result will show an intrinsic robustness which makes it insensitive to all "random" local variations in resistances as well as in local diode properties; such inhomogeneities will be discussed subsequently (Section 8). For this linearized description, the standard equivalent circuit model, Figure 1a, is replaced by that of **Figure 2**a with a lumped diode resistance R_D (differential resistance of the ideal lumped I–U characteristic), which is related to K by

$$KA = \frac{1}{R_\mathrm{D}} \cong \frac{q}{kT}\overline{I}_\mathrm{D} \tag{9}$$

i.e., $\overline{U}_\mathrm{D}$ is the diode voltage which leads to the total dark current $\overline{I}_\mathrm{D}$. So, for each working point along the I–U curve, a different value for K must be used in the following. The relation between the lumped series resistance R_s of the equivalent circuit and the sheet resistivity ρ_sh will be derived subsequently. The linearized version of the local distributed network in Figure 1b is shown in Figure 2b.

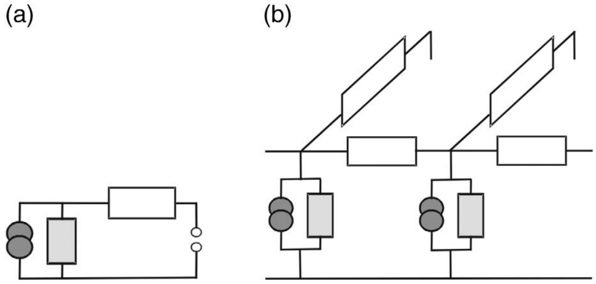

Figure 2. a) Linearized equivalent circuit diagram corresponding to Figure 1a, with photocurrent source (medium gray), linearized diode resistance R_D [light gray; cf. Equation (9)], and series resistance R_s (white); b) linearized version of Figure 1b [same symbols as in (a)].

For our series-resistance analysis, we consider the simplest geometry that comprises all relevant "2D features" of a series-resistance network and which is fully analytically treatable. However, the results of this model geometry can be quite easily generalized to facilitate general statements valid for all large-area solar cells for which lateral current flow has a relevant influence on the lateral voltage distribution. To that end, a circular solar cell with a constant emitter sheet resistivity ρ_sh and a metal contact at the edge as shown in **Figure 3** is used, originally introduced in ref. [3]. Here, we additionally discuss explicitly the photocurrent influence and present the calculation in more detail (see also the Analytical Section in the Supporting Information). This geometry aims at modeling the basic 2D features of a large-area silicon solar cell, namely the laterally distributed series resistance; the base bulk resistivity ρ_b is neglected in the mathematical model, but later on considered by a lumped nondistributed series resistance. As we will see from the results, the circular geometry (chosen to enable a fully analytical treatment) is not a restriction for the application to real solar cells.

5. Lumped Series Resistance: Definition and Variational Expression

Due to its robustness and versatility,[66] the standard procedure to determine the lumped series resistance for any given dark diode forward current is

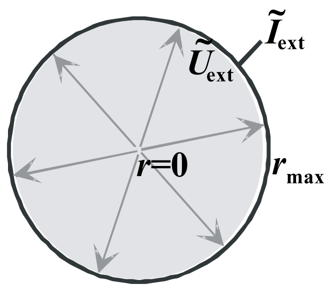

Figure 3. Simple 2D solar cell model (top view), described by a constant emitter sheet resistivity ρ_sh and a laterally homogeneous area-related diode conductivity K (in vertical direction, indicated by the light gray plane [cf. Figure 2]). The boundary values for the variational quantities $\widetilde{I}_\mathrm{ext}$ and $\widetilde{U}_\mathrm{ext} = \widetilde{U}(r_\mathrm{max})$ are indicated. The rotational symmetry is chosen to enable a fully analytical treatment.

© 2019 The Authors. Published by WILEY-VCH Verlag GmbH & Co. KGaA, Weinheim

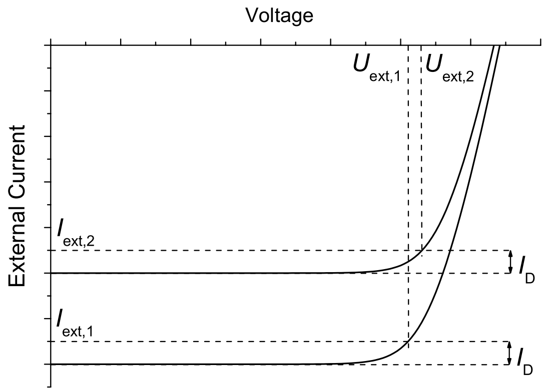

Figure 4. Schematic illustration of the quantities used in Equation (10) to determine the lumped series resistance according to the two-light-level method; the chosen dark current I_D is identical for both illumination levels.

$$R_s := \frac{U_{ext,2} - U_{ext,1}}{I_{ext,2} - I_{ext,1}} \tag{10}$$

where the indices 1 and 2 refer to two different levels of illumination and working points having identical total dark current for both illumination levels ("double illumination method" or "two light level method"[37,39,41] or, more generally, "multi-light method"[41] or "illumination intensity variation method"[52]; cf. **Figure 4**). We are aware that in the literature there are also other ways to define the lumped series resistance; however, the present definition is the most meaningful one, as it is directly related to an unambiguous measurement prescription, and it is least influenced by material-related injection-level dependencies. Later on we will provide further reasons why only this way of measuring it makes the lumped series resistance a physically sensible parameter.

For our variational formalism, Equation (10) means that the very same lumped series-resistance result is obtained by

$$R_s = \frac{\widetilde{U}_{ext}}{\widetilde{I}_{ext}} \tag{11}$$

for constant I_D, i.e., for $\widetilde{I}_D = 0$. This enforces a certain dependence between $\widetilde{U}_{ext}$ and $\widetilde{I}_{ext}$ which will now be derived. In our model, the external contact is at the edge of the circular solar cell, for which $r = r_{max}$. Treating the homogeneous photocurrent variation as a voltage offset, we split $\widetilde{U}$ into U^* and this offset [cf. Equation (A6) in the Analytical Section in the Supporting Information]

$$\widetilde{U}_{ext} = \widetilde{U}(r_{max}) = U^*(r_{max}) + \frac{\widetilde{J}_{ph}}{K} \tag{12}$$

We define the auxiliary function (whose meaning will be discussed subsequently)

$$R(r) := \frac{U^*(r)}{\widetilde{I}_{ext}} \tag{13}$$

so Equation (12) becomes, using R_D from Equation (9) and $\widetilde{I}_{ph} = \widetilde{J}_{ph} A$

$$\widetilde{U}_{ext} = R(r_{max})\widetilde{I}_{ext} + R_D \widetilde{I}_{ph} \tag{14}$$

This shows how, in general, a change in the external voltage is related to independent values of the current variations $\widetilde{I}_{ext}$ and $\widetilde{I}_{ph}$. For the lumped series-resistance determination according to Equation (11), however, $\widetilde{I}_D = 0$ is mandatory, so there is no such independence, then: From the general current conservation relation, $I_{ext} = I_D - I_{ph}$, we have that

$$0 = \widetilde{I}_D = \widetilde{I}_{ext} + \widetilde{I}_{ph} \tag{15}$$

so that, self-evidently

$$\widetilde{I}_{ext} = -\widetilde{I}_{ph} \tag{16}$$

must be chosen for the series-resistance determination, i.e., any variation in the photocurrent must exactly be compensated by a corresponding change in the external current to keep the diode current constant. Inserting this into Equation (14), we have from the fundamental series-resistance definition, Equation (11), that

$$R_s = R(r_{max}) - R_D \tag{17}$$

Provided that the equivalent circuit holds, this expression can be understood from Figure 2a: For zero photocurrent, the voltages at series resistance and diode resistance sum up, so that series resistance equals total resistance minus diode resistance. That $R(r_{max})$ indeed represents the total resistance follows from being derived from $U^*(r_{max})$, which equals $\widetilde{U}_{ext}$ for $\widetilde{I}_{ph} = 0$. However, at this point we mention already that, although Equation (17) always yields a certain numerical value with the unit of measurement of ohm, not always does it make sense to represent it by an ohmic resistor, i.e., the formal validity of Equation (17) extends beyond that of the standard equivalent circuit model. We will show this in Section 7.

To use Equation (17) in a series-resistance determination, the quantities on its right-hand side have to be accessible in a measurement. We show that this is indeed the case by elucidating the meaning of $R(r)$: In general, using the principle of current conservation as expressed by Equation (A13) in the Analytical Section in the Supporting Information, one has for the average of $R(r)$ over the circular area A that

$$\frac{1}{A}\int_0^{2\pi}\int_0^{r_{max}} R(r')\, r'\mathrm{d}r'\mathrm{d}\varphi = \frac{2\pi}{A\widetilde{I}_{ext}}\int_0^{r_{max}} U^*(r')r'\mathrm{d}r' = \frac{1}{KA} = R_D \tag{18}$$

i.e. $R(r)$ expresses a "quasi-local" (radius-dependent) diode resistance. Furthermore, we note that, since Equation (18) relates the diode resistance R_D to the average value of the offset-corrected voltage variation $U^*(r)$, this offers the possibility to avoid the purely theoretical way of introducing the diode conductivity K via Equation (7): Using the photocurrent substitution [given by Equation (A6)] in Equation (18), we arrive at

$$R_D = \frac{1}{\widetilde{I}_{ext} + \widetilde{I}_{ph}}\frac{2\pi}{A}\int_0^{r_{max}} \widetilde{U}(r')r'\mathrm{d}r' \tag{19}$$

© 2019 The Authors. Published by WILEY-VCH Verlag GmbH & Co. KGaA, Weinheim

i.e., for a given excitation via $\tilde{I}_{\text{ext}} + \tilde{I}_{\text{ph}}$, the resulting average voltage response—which is a measurable quantity—is a measure for the diode resistance. It will turn out that also for our local series-resistance definition to be sensible, it is important that R_{D} is a measurable quantity—more precisely: measurable without having to know the series resistance.

Here we come back to the discussion from Section 2 where we emphasized that voltages cannot be averaged because voltage is not an extensive property. However, the effective voltage averaging that we arrived at in Equation (19) comes from the conservation of all vertical currents, and as we here describe the p–n forward junction current in a linear approximation using a constant K, summing up all vertical currents is mathematically equivalent to summing up the local voltages [cf. Equation (A13)].

Altogether, this means that all information necessary to obtain the lumped series resistance is contained in the auxiliary function $R(r)$, Equation (13), or—equivalently—in the offset-corrected variational voltage distribution $U^*(r)$ [whose full solution for the circular model is given in the Analytical Section in the Supporting Information, Equation (A16)]. Therefore, to obtain the lumped series resistance—and, as will be described later, also the local series resistance—for arbitrary grid geometries, it suffices to calculate the variational response for the respective linearized problem, i.e., one just has to solve the relevant Helmholtz equation derived from Equation (6) by introducing the linearization for the diode current; for the circular model, this is Equation (A12) in the Analytical Section in the Supporting Information.

As according to Equation (10), only two different pairs of current–voltage measurements for identical diode current are needed and no full I–U characteristic, the finding of Equation (17) is a general result; it holds independently of the validity of the standard equivalent circuit. That the series resistance resulting from Equation (17) is valid just for a certain dark current, leading to a specific value of the diode resistance R_{D}, and since different values for the series resistance R_{s} might be obtained for different dark currents, is one reason why it does not always make sense to represent a such-obtained value by a standard ohmic resistor in the equivalent circuit. A further reason is that an ohmic resistor leads to Joule losses according to the simple expression $P = RI^2$. However, in the general case this is not fulfilled for the distributed series resistance; this is explicitly shown in the second part of the Analytical Section in the Supporting Information. The main result obtained there is that only for a voltage distribution which can be described in linear order in the sheet resistivity ρ_{sh}, the variational series-resistance expression, Equation (17), yields a quantity for which it is justified to be represented by an ohmic resistor in the equivalent circuit, as only then the distributed Joule losses add up to the lumped value (which is the fundamental condition raised by Micard and Hahn[56]), making R_{s} a physically sensible parameter.

Luckily, this purely theoretical concept ("can be described in linear order in the sheet resistivity ρ_{sh}") has a consequence which permits to identify from local solar cell measurements the validity of this "description in linear order" for a given solar cell; this is discussed in detail in the following Section.

6. Local Series Resistance: Definition and Properties

In this Section, we present our definition of a local series resistance in detail. The starting point is the auxiliary function $R(r)$ as defined in Equation (13). We have from the full solution for the circular model, Equation (A16), that

$$R(r) = \frac{\sqrt{\rho_{\text{sh}}}}{2\pi r_{\max}\sqrt{K}} \frac{I_0(\sqrt{\rho_{\text{sh}}K}r)}{I_1(\sqrt{\rho_{\text{sh}}K}r_{\max})} \tag{20}$$

with the modified Bessel functions of the first kind of order zero and one, I_0 and I_1. In general, $R(r)$ is a measurable quantity; it can be obtained from luminescence images[11,60] or from CELLO maps.[3,67] We now introduce a "quasi-local" (strictly speaking: radius-dependent) series-resistance function by defining

$$R_{\text{s}}(r) := R(r_{\max}) - R(r) \tag{21}$$

This definition has two important consequences which justify the choice for $R_{\text{s}}(r)$: 1) $R_{\text{s}}(r)$ is a positive-valued function; 2) the arithmetic average of $R_{\text{s}}(r)$ leads exactly to the variational expression for the lumped series resistance, Equation (17)

$$\langle R_{\text{s}}(r)\rangle = R(r_{\max}) - \langle R(r)\rangle = R(r_{\max}) - R_{\text{D}} = R_{\text{s}} \tag{22}$$

[cf. Equation (18) for the average of $R(r)$]. Inserting the explicit expression for $R(r)$, Equation (20), we obtain the already-announced relation between the lumped series resistance and the sheet resistivity ρ_{sh} for the circular model [using $r_{\max} = \sqrt{A/\pi}$ and Equation (9)]

$$R_{\text{s}} = \frac{\sqrt{\pi\rho_{\text{sh}}R_{\text{D}}}}{2\pi} \frac{I_0\left(\sqrt{\frac{\rho_{\text{sh}}}{\pi R_{\text{D}}}}\right)}{I_1\left(\sqrt{\frac{\rho_{\text{sh}}}{\pi R_{\text{D}}}}\right)} - R_{\text{D}} \tag{23}$$

The "quasi-local" series-resistance definition, Equation (21), can easily be extended to yield a full local series-resistance map for usual solar cells (cf. refs. [3,11,60,67,68]): Provided that a map of the auxiliary function $R(x, y)$ exists with the property corresponding to Equation (18), i.e., that its arithmetic average, $\langle R(x, y)\rangle$, equals the diode resistance R_{D} of the working point for which this map was taken, the local series resistance is given by

$$R_{\text{s}}(x, y) = R_{\max} - R(x, y) \tag{24}$$

with $R_{\max}$ being the maximum value of the $R(x, y)$ data. By construction, also this definition leads to the averaging property expressed by Equation (22), i.e., the arithmetic average of the local series resistances, $\langle R_{\text{s}}(x, y)\rangle$, equals the lumped series resistance R_{s} as given by the two-light-level method.

As mentioned at the end of Section 5, only for a voltage distribution that can be described in linear order in the sheet resistivity ρ_{sh}, the equivalent circuit holds, because only then the Joule losses are correctly described by the lumped R_{s} represented by an ohmic resistor. Thus, the linear order in the sheet resistivity is of special importance, and because of this (and of its experimental relevance, see below), we now investigate this case in further detail. Solving the fundamental differential equation of the

© 2019 The Authors. Published by WILEY-VCH Verlag GmbH & Co. KGaA, Weinheim

circular model, Equation (A12), up to linear order in ρ_{sh} is equivalent to use a lowest-order polynomial approximation to I_0 in the general solution, Equation (A14), according to

$$I_0(x) \cong 1 + \frac{x^2}{4} + \frac{x^4}{64} + \ldots \tag{25}$$

which, according to Equation (23), requires $\rho_{sh}/(\pi R_D) < 1$, i.e., to be in the regime linear in ρ_{sh} is only possible for the diode resistance being large compared with the sheet resistivity; this result was independently obtained already by Boone and van Doren.[49]

In what follows, we use the abbreviation

$$a := \frac{\pi r^2}{A} \tag{26}$$

for the area fraction of the solar cell inside the radius r; a is referred to, for short, as the fractional area. Applying the external boundary condition, Equation (A13), to the general solution linear in ρ_{sh}, Equation (B7a) in the Analytical Section in the Supporting Information, we get

$$R_1(a) = R_D \frac{1 + \frac{1}{4}\frac{\rho_{sh}}{\pi R_D} a}{1 + \frac{1}{8}\frac{\rho_{sh}}{\pi R_D}} \tag{27}$$

the index "1" referring to stemming from the linear order in ρ_{sh}. Due to the factor R_D Equation (27) explicitly shows that $R_1(a)$ expresses a "local" (fractional-area-related) diode resistance. Clearly, since $R_1(a)$ depends linearly on a and a varies between 0 and 1, the average of $R_1(a)$ is attained at $a = 0.5$, i.e., $\langle R_1(a) \rangle = R_1(0.5)$, and from Equation (27) one has that $\langle R_1(a) \rangle = R_D$ [cf. Equation (B12) in the Analytical Section in the Supporting Information for averages taken over a]. From Equation (17) one has that, in terms of the fractional area, the lumped series resistance can be obtained as $R_s = R(1) - R_D$, and analogously to Equation (21), the fractional-area-related series resistance is

$$R_{s,1}(a) := R_1(1) - R_1(a) \tag{28}$$

Since $R_1(a)$ shows a linear behavior, so does $R_{s,1}(a)$. **Figure 5** shows these results.

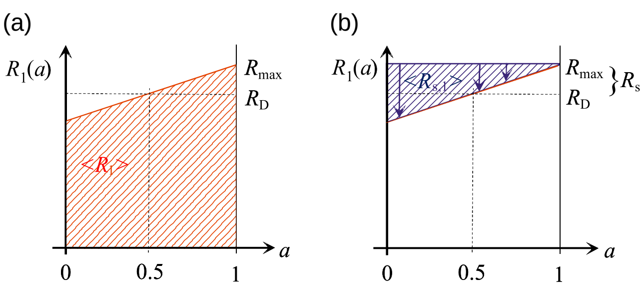

Figure 5. a) Illustration of Equation (27) with linear-order local diode resistance $R_1(a)$ versus fractional area a. The average of the local diode resistance equals the lumped diode resistance, $\langle R_1(a) \rangle = R_D = R_1(0.5)$. b) Illustration of Equation (28) with $R_1(a)$ (red line) and linear-order local series resistance $R_{s,1}(a)$ (downward blue arrows) versus a and indicating the calculation of the linear-order lumped series resistance $\langle R_{s,1}(a) \rangle$ according to Equation (22).

From the general definition of the auxiliary function R, Equation (13), we have that for the here-considered case of the solution linear in the sheet resistivity ρ_{sh}, the offset-corrected variational voltage distribution across the solar cell area is given by

$$U_1^*(a) = R_1(a)\,\tilde{I}_{ext} = R_D \tilde{I}_{ext} \frac{1 + \frac{1}{4}\frac{\rho_{sh}}{\pi R_D} a}{1 + \frac{1}{8}\frac{\rho_{sh}}{\pi R_D}} \tag{29}$$

i.e., the voltage varies linearly across the area of the solar cell. This can be directly checked experimentally: For example, for a CELLO voltage map, it suffices to analyze the histogram of the map data to check for a linear distribution across the solar cell area. The technicalities of this method were already discussed in detail in several publications[3,60,67,69]; it can equally well be applied to voltage images obtained from luminescence measurements. Here, we emphasize the relevance of this check: Only if the voltage distribution across the solar cell area can be described in linear order in ρ_{sh}, i.e., only when the voltage varies linearly across the area of the solar cell, the equivalent circuit—and, therefore, a fit of the I–U characteristic to an expression resulting from the standard equivalent circuit—makes sense at all.

We have routinely checked the distribution of the voltage across the area of a solar cell through the years for a number of solar cells, and for standard industrial large-area silicon solar cells (i.e., "properly designed"[49] ones) this has always been found to be linear. This linearity was previously introduced as a criterion for "economically reasonable"[69] solar cells. Compared with the circular solar cell model studied here, at first glance it might be surprising that for a real solar cell the voltage should vary linearly across the solar cell area, because in each lateral direction, the dependence of the voltage is (to a very good approximation) quadratic in the respective Cartesian coordinate. However, for a standard industrial large-area silicon solar cell with an H-type grid, this leads to the equipotential lines between busbars and grind fingers being ellipses, which gives the linear scaling with the area.

At this point, we want to discuss the peculiarities of the solution that we have obtained so far: We have solved the Helmholtz equation, Equation (A12), obtained for not-too-large lateral voltage variations by a linearization with respect to the diode current from the general equation for the local emitter voltage, Equation (6). The latter contains second-order spatial derivatives and, most importantly, a nonlinear dependency on the local voltage; note that because of this nonlinearity, it is not a proper Poisson equation, although it looks like it at the first glance. Most importantly, due to this nonlinearity, its solution "naturally" contains effects nonlinear in ρ_{sh}. In contrast, we have provided a simplified solution of the Helmholtz equation which is in linear order in ρ_{sh}, and we have identified this to be the "natural" regime on standard industrial ("properly designed"/"economically reasonable") solar cells.

We stress the relevance of the latter in more physical terms: The general equation for the local emitter voltage, Equation (6), incorporates the feedback between the voltage and the current distribution, leading to a full-order self-consistency between current and voltage distributions—however, there is no such feedback on standard industrial solar cells (cf. the second part

© 2019 The Authors. Published by WILEY-VCH Verlag GmbH & Co. KGaA, Weinheim

of the Analytical Section in the Supporting Information): The current distribution relevant for the voltage distribution in linear order in ρ_{sh} is the one for the case of vanishing series resistance.

Therefore, applying directly the general, nonlinear equation to the measured voltage distribution of a solar cell (as done in some studies dealing with luminescence imaging of large-area silicon solar cells, e.g., refs. [10,19,20,70]) effectively means to look for a solution intrinsically nonlinear in ρ_{sh}, incorporating the aforementioned feedback between voltage and current. However, in this way, the dominating feedback-free voltage distribution on a standard industrial solar cell—which, as discussed earlier, is in linear order in ρ_{sh}—is hard to find; this also illustrates why the measurement noise has a drastic influence on the aforementioned studies. In our LR-R_s approach, we avoid these noise problems as we only consider the voltage distribution in linear order in ρ_{sh}.

In the linear case [cf. Equation (27) and (28)], it is easy to verify that all local Joule losses sum up to $P_s = R_{s,1} I_{ext}^2$ (as discussed by Micard and Hahn[56] as well as by van der Heide and Poortmans[57]); this is explicitly shown in the second part of the Analytical Section in the Supporting Information. It is an important check for the series-resistance network of real solar cells as the full solution, Equation (20), does not fulfill this condition in general, which is also shown in the Analytical Section in the Supporting Information. There it is additionally shown that already for the quadratic order in ρ_{sh} the equivalent circuit is not compatible with the Joule losses, i.e., it is invalid with respect to the Joule losses. This is why, for "properly designed"/ "economically reasonable" large-area silicon solar cells, it is sufficient to consider distributed series-resistance effects in linear order in ρ_{sh}.

In contrast, in the model of independent diodes there is no low-ohmic lateral coupling, hence orders in ρ_{sh} cannot be defined in this model at all. This clearly shows that this model is unsuited for large-area silicon solar cells. Instead, this model only works in cases of dominating ohmic losses due to vertical current flow through many similar parallel current paths. Then, the relevant description is that by a lumped conductance, which is given by the arithmetic mean of the conductances of the various paths; i.e., the physically meaningful series-resistance average is then given by the harmonic mean (reciprocal of the arithmetic mean of the reciprocals) of the path resistances; in this way, it was introduced in ref. [1].

Originally, the model of independent diodes was already implicitly contained in the work by Boone and van Doren.[49] Later, it was explicitly formulated by Mijnarends et al.[59] and Rau et al.[61] for the description of larger areas (classes of crystallites) of inhomogeneous solar cells, and it was stated that "the currents in the circuits of the individual crystallites are independent."[59] However, these areas are determined by selecting sites with similar properties, making each of these areas for themselves more homogeneous than the whole solar cell. Yet, this implies that the coupling effects between these areas are the largest occurring on that solar cell, possibly violating the assumed independence. Moreover, when applied in a case where lateral currents dominate the voltage distribution (and the influence of bulk resistances can be neglected), another problem inherent to the model of independent diodes, with the harmonic mean being its "natural" average, is revealed: For vanishing sheet resistivity, $\rho_{sh} \to 0$, this averaging rule, $R_s^{-1} = N^{-1} \sum_{(x,y)} R_s^{-1}(x,y)$, breaks down because, when all resistances go to zero, the terms under the sum diverge. Because, as discussed in Section 3, $\rho_{sh} \to 0$ is the "natural limiting case" for large-area silicon solar cells, this again shows that the model of independent diodes is unsuited for such cells.

Finally, we mention that, following Ramspeck et al.[4] in just doing so, meanwhile, it is common to use the arithmetic mean also for the model of independent diodes when applied to large-area silicon solar cells, with rather reasonable results,[5,54] yet without any physical substantiation. From our theory, it can at best be understood why also in this model a reasonable arithmetic average is obtained; this will be discussed in Section 8. However, there are further arguments why the model of independent diodes does not fit to large-area silicon solar cells at all, and why it cannot be derived from Ohm's law and the continuity equation (in contrast to what was mentioned in ref. [54]); for details see the relevant discussion in ref. [68].

7. Dark-Current Dependence of the Series Resistance

For reasons becoming clear below, we define

$$R_{s,\infty} := \frac{1}{8}\frac{\rho_{sh}}{\pi} \tag{30}$$

by which, we can rewrite Equation (27) as

$$R_1(a) = R_D \frac{1 + \frac{2R_{s,\infty}}{R_D} a}{1 + \frac{R_{s,\infty}}{R_D}} \tag{31}$$

which for the lumped linear-order series resistance $R_{s,1} = R_{max} - R_D = R_1(1) - R_1(0.5)$ yields

$$R_{s,1} = \frac{R_{s,\infty}}{1 + \frac{R_{s,\infty}}{R_D}} \tag{32}$$

or, equivalently

$$\frac{1}{R_{s,1}} = \frac{1}{R_{s,\infty}} + \frac{1}{R_D} \tag{33}$$

This means that the series resistance is not constant but varies with the total dark current $\bar{I}_D$ defining the working point, since the latter determines the corresponding diode resistance R_D: The more the considered working point lies in forward direction, the larger the dark current and, thus, the smaller R_D [cf. Equation (9)]—and therefore also the smaller the lumped series resistance. This is the main consequence of the fact that the solar cell's lumped series resistance results from a distributed network: For large-enough forward bias, the p–n junction acts as a bypass, reducing the ohmic losses in the grid and the emitter as a larger fraction of current leaves the emitter, resulting in an effectively shorter traveling distance in the emitter. For low forward bias, the bypass is blocked, and the lumped series resistance equals the limiting value $R_{s,\infty}$, with its label referring to "infinite" diode resistance. The same expression for this limit [Equation (30)]

© 2019 The Authors. Published by WILEY-VCH Verlag GmbH & Co. KGaA, Weinheim

is known already from a calculation for the same geometry and explicitly referring to short-circuit conditions.[71]

So, according to Equation (32), for all working points, a single parameter R_s exists that represents the lumped series resistance, with its variation along the I–U curve being fully described by the dark-current dependence inherent in the diode resistance R_D [cf. Equation (9)]. The variation of the lumped series resistance along the I–U curve was experimentally observed already by Wolf and Rauschenbach[37] as early as in 1963 using the two-light-level method; it was further investigated in several works: experimentally, e.g., in refs. [11,38–41,60,63,67,72–74], analytically, e.g., in refs. [3,45–47,63,75,76], and numerically, e.g., in refs. [39,42,45–48,63,75,76]. Compared to the analytical literature works on this subject, our result [Equation (33)] is much simpler. As we mentioned earlier in the Introduction, there is experimental evidence that the actual solar cell behavior is indeed that simple.[42] Here, we additionally mention that this simplicity is not an artifact of the circular geometry: Both in a precedent work for an effective 1D geometry[77] and recently also in a 2D description for an H-type grid geometry,[68] we obtained a similarly simple expression for the dark-current dependence of the lumped series resistance.

Furthermore, note that in the literature frequently an ansatz is found that describes R_s as being dependent on the external current, i.e., on the strength of the current flowing through R_s itself (cf., e.g., refs. [41,46,54,63]). Such an ansatz, however, makes the series resistance of a solar cell an intrinsically nonlinear element, which is against all what "ohmic series resistance" stands for. So, it would need a fundamental justification and thorough experimental verification that this is the only way to handle the series-resistance behavior of a large-area silicon solar cell—which, however, is not provided in the relevant literature.

At this point, we want to emphasize again that we have obtained the effect of a dark-current-dependent series resistance for the case of a voltage distribution in linear order in ρ_{sh}, which is an order where the whole solar cell area contributes unrestrictedly to the external current since, as mentioned earlier (Section 6), for the voltage distribution in linear order in ρ_{sh}, the relevant current distribution is in zeroth order in ρ_{sh}. We stress the relevance of the latter in more physical terms: In this order in ρ_{sh}, no area loss occurs. Therefore, an observation of a decrease in the lumped series resistance at increased dark current does not necessarily mean that area loss had occurred.

As a consequence of the lumped series resistance depending on the dark current flowing, using a series-resistance determination method working at fixed dark current—as does the two-light-level method—is the only meaningful way to define the lumped series resistance for large-area silicon solar cells. Thus, we claim that also for local series-resistance measurements, it is necessary to keep the total dark current constant because, if the average of a certain local series-resistance image/map does not equal the relevant lumped R_s value for the dark current used, this image/map does not correctly represent the local series resistance. Therefore, if the local series-resistance data are not obtained from measurements that use the same dark current (cf., e.g., ref. [12]), those data might be untrustworthy; it is much safer to use data obtained from measurements made at constant dark current.

Also, we claim that it is even sufficient to keep the total dark current constant for the local series-resistance measurement, because this corresponds to "natural" operating conditions of a large-area solar cell. For the case of luminescence-imaging-based measurements, we have made the experience that a quite robust way to experimentally fulfill the condition of constant total dark current is to choose measurement conditions with the same average luminescence intensity for taking the relevant images.[73] We note that, instead, in the luminescence-imaging-based local series-resistance measurement method by Kampwerth et al., the local dark current is kept constant.[6] However, in this method, this is achieved by a variation of the cell voltage during the measurement of a single image; therefore, the resulting image does not refer to a "natural" operating condition of a large-area solar cell. Moreover, this concept is a significantly less robust method for the investigation of solar cells with locally severe series-resistance problems than to keep the total dark current constant.

8. Generalization of the Distributed Series Resistance Model

The transition from the full solution, Equation (20), to (27), i.e., the linearization with respect to ρ_{sh}, can be directly performed in the integro-differential Equation (A11) given in the Analytical Section in the Supporting Information, facilitating a much deeper insight into the physical meaning of the linearization. Using the variable a (fractional area) instead of r (radius)—which, according to Equation (26), leads to the substitution $\mathrm{d}a/\mathrm{d}r = 2\sqrt{\pi a/A}$—in Equation (A11), we have

$$\frac{\mathrm{d}U^*}{\mathrm{d}a} = \frac{\rho_{sh} KA}{4\pi}\frac{1}{a}\int_0^a U^*(a')\mathrm{d}a' \tag{34}$$

This facilitates to hierarchically derive solutions for the offset-corrected variational voltage $U^*(a)$ in different orders of ρ_{sh}. The solution in zeroth order in ρ_{sh} (i.e., for vanishing ρ_{sh}) is just $\mathrm{d}U_0^*/\mathrm{d}a = 0$, i.e., $U_0^* = \text{const} = R_D\tilde{I}_{ext}$ (for details see the second part of the Analytical Section in the Supporting Information). Due to the prefactor on the right-hand side of Equation (34), to get the solution in linear order in ρ_{sh}, one just has to replace $U^*(a')$ by U_0^* in the integral of Equation (34), i.e.

$$\frac{\mathrm{d}U_1^*}{\mathrm{d}a} = \frac{\rho_{sh} KA}{4\pi}\frac{1}{a}\int_0^a U_0^*\,\mathrm{d}a' \tag{35}$$

As a consequence of the factor $1/a$ in front of the integral, $\mathrm{d}U_1^*/\mathrm{d}a$ is constant, thus clearly leading to the simplified solution of Equation (27). Please note that the factor $1/a$ in front of the integral is a direct consequence of the model being 2D; in the corresponding 1D equation, there is no such normalizing factor, cf. Equation (A-6) in ref. [77]. The physical reason for this factor is the increased number of paths to points far away from the contacts, thereby compensating the increased ohmic losses along one path.

Equation (35) thus can be interpreted in a second way: A part of Equation (34), namely

© 2019 The Authors. Published by WILEY-VCH Verlag GmbH & Co. KGaA, Weinheim

$$\langle \tilde{I}_z \rangle(a) := KA\frac{1}{a}\int_0^a U^*(a')\,\mathrm{d}a' \tag{36}$$

just describes averages over net local junction currents [cf. Equation (A7) in the Analytical Section in the Supporting Information]. In zeroth order, this average is constant and equals U_0^*/R_D. Including the latter in Equation (35) and using the limiting value $R_{\mathrm{s},\infty}$ [Equation (30)], we find

$$\frac{\mathrm{d}U_1^*}{\mathrm{d}a} = 2R_{\mathrm{s},\infty}\left\langle \tilde{I}_z \right\rangle = 2\frac{R_{\mathrm{s},\infty}}{R_\mathrm{D}}U_0^* \tag{37}$$

Due to this dependence on the average junction current, in linear order in ρ_sh, the solution and all consequences described in the previous Sections will not differ if, e.g., local diode properties vary randomly from point to point (i.e., distributed according to white unbalanced noise) or if local series resistance and local diode properties are spatially uncorrelated, i.e., in cases where

$$\left\langle \left\{ \tilde{I}_z(x,y) - \left\langle \tilde{I}_z \right\rangle \right\} \left\{ R_\mathrm{s}(x,y) - \langle R_\mathrm{s} \rangle \right\} \right\rangle = 0 \tag{38}$$

As such a situation can be found on multicrystalline (mc-Si) cells, this motivates to apply our theory also to such cells albeit that they do not fulfill the premise of a constant K. Note that the latter, however, was just a mathematical means to solve the equations; the relevant physics was then identified to be the linearity of the voltage distribution with respect to ρ_sh, which can hold for mc-Si cells as well; the inhomogeneities in the diode properties manifest themselves mainly in additional lateral currents in the emitter sheet. Therefore, it is fully left to the experiment to test the validity of our LR-R_s approach for any given solar cell.

These findings can be generalized for arbitrary grid geometries: For any solar cell having a voltage distribution in linear order in ρ_sh, the current cannot depend on ρ_sh. This implies that a sheet current distribution occurs as if ρ_sh were zero, and by flowing through the series-resistance network, this current builds up the lateral voltage distribution over the solar cell area. Note that this explains an approach for the description of series-resistance effects used in the literature already for a long time (as, e.g., in ref. [78]): that for good solar cells, R_s mainly leads just to a voltage drop but not to a change in current.

Equations (36) and (38) can explain why local diode variations have a much less severe influence on local series resistances than often expected. A further reason for the quasi-insignificance of varying local diode properties for the series-resistance behavior of a large-area silicon solar cell is the existence of lateral balancing currents over short distances: As long as the approximation of ohmic losses up to linear order in ρ_sh is valid even for the whole solar cell, ohmic losses for lateral balancing currents over short distances are negligible. (The real challenge are lateral balancing currents over large distances across a solar cell; however, they will be treated in a separate work.) It was probably due to all this why the "model of independent diodes" as described, e.g., in refs. [59,61] (and later used in many works, e.g., in refs. [1,2,4,5,7–10,12–17,19,27,29,30,34,54]) could be applied to large-area silicon solar cells without running into difficulties, while also leading to a reasonable arithmetic average.

In the here-treated analytical model, having rotational symmetry, lateral voltage differences (i.e., ohmic losses) in first order can, by using Equation (35), be expressed as

$$U_1^*(a_2) - U_1^*(a_1) = \int_{a_1}^{a_2} \frac{\mathrm{d}U_1^*}{\mathrm{d}a}\,\mathrm{d}a' = \frac{1}{4\pi}\frac{U_0^*}{R_\mathrm{D}}\int_{a_1}^{a_2} \rho_\mathrm{sh}\,\mathrm{d}a' \tag{39}$$

This shows the robustness of the 2D network: Ohmic losses even for nonconstant ρ_sh can still be obtained easily, and they scale with the average ρ_sh along the respective path.

Some essential differences exist for the 1D case. The factor corresponding to $1/a$, which would be $1/x$, is missing in the equations corresponding to Equation (34)–(36); thus, $\mathrm{d}U^*/\mathrm{d}x$ scales with x, i.e., the voltage $U_1^*(x)$ linear in ρ_sh scales with x^2 (cf. Appendix A in ref. [77]). So while in the 1D case—more precisely, for an area A laterally homogeneous along the length l—$\mathrm{d}U^*/\mathrm{d}a = (A/l)\mathrm{d}U^*/\mathrm{d}x$ scales with the integral of local diode currents, in the 2D case $\mathrm{d}U^*/\mathrm{d}a$ scales with the average of local diode currents. This leads to a significant influence in the position of local recombination-active defects on ohmic losses in the 1D case, which does not exist in the 2D case. Additionally, unambiguous averaging of diode properties is not possible in 1D because their relevance for the lumped solar-cell properties drastically depends on the position relative to the grid; if, e.g., a grid finger is broken in the 1D case, all diodes beyond that point do not contribute to the lumped solar-cell properties. In the 2D case, a broken grid finger just leads to an increased current flow along ways bypassing the broken grid finger.

In summary, the factor $1/a$ in front of the integrals in Equation (34) and (35) reflects the intrinsic robustness of a 2D network for bypassing grid defects. Current flow across a 2D network is a strongly distributed phenomenon, and this is necessary to apply reasonably the standard equivalent circuit shown in Figure 1a to "properly designed"/"economically reasonable" silicon solar cells containing inhomogeneities. The lateral 2D current flow introduces a robustness into map averaging, which is the fundamental reason why so often the standard equivalent circuit describes "properly designed"/"economically reasonable" silicon solar cells so well.

9. Equivalent Circuit Including the Effect of the Distributed Series Resistance

Equation (32) and (33) describe just the distributed part of the series resistance of a solar cell, and they are valid only for the circular model. For real solar cells with an H-type grid geometry, a similar calculation also results in the inverse of the distributed series resistance depending linearly on $1/R_\mathrm{D}$, but with a different factor[68]; the details will be given elsewhere. Generalizing these findings, to take also other grid geometries into account, instead of Equation (33) one has

$$\frac{1}{R_\mathrm{s}^\mathrm{dist}} = \frac{1}{R_{\mathrm{s},\infty}} + g\frac{1}{R_\mathrm{D}} \tag{40}$$

where g is a constant depending just on the geometry of the series-resistance network. The series resistances resulting from main busbars, the back contact and the bulk resistance introduce

© 2019 The Authors. Published by WILEY-VCH Verlag GmbH & Co. KGaA, Weinheim

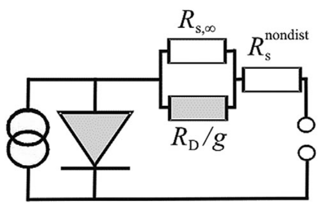

Figure 6. Equivalent circuit according to Equation (41). The light gray resistance is the dark-current-dependent diode resistance R_D divided by the geometry factor g, whereas the white resistances represent the globally constant series resistances.

nondistributed (i.e., homogeneous) ohmic losses, so the complete lumped series resistance of the solar cell, $R_s = R_s^{dist} + R_s^{nondist}$, can be written as

$$R_s = \frac{1}{\frac{1}{R_{s,\infty}} + \frac{g}{R_D}} + R_s^{nondist} \tag{41}$$

This expression leads to the equivalent circuit shown in **Figure 6**. This equivalent circuit, in combination with the simultaneous averaging procedure for local series and diode resistances as described earlier (Section 6), leads to consistent and completely quantitative results for mono- and many multicrystalline solar cells investigated using the CELLO[3,67] as well as photoluminescence[11,42,60,73] techniques.

As a practical consequence, note that the fact that the series resistance depends on the dark current points to an issue for the investigation of injection-level dependencies: Unless an I–U measurement is corrected for the dark-current dependence of the series resistance, the latter may invalidate the interpretation of an observed injection dependence of other solar cell properties derived from the I–U measurement. Moreover, even without injection-level dependence, the numerical values and the fit quality of standard I–U curve parameters can vary with the way the series resistance is treated: Taking the variation of R_s into account can considerably improve the fit quality, increasing the accuracy of all results.[41]

Vice versa, not taking the variation of R_s along the I–U curve into account can lead to certain phenomena not being identified as systematic errors; e.g., measuring the series resistance based on a fit to the dark I–U curve in the high-current regime leads to systematically lower R_s values, which was mistakenly considered to be a general property of $R_{s,dark}$.[52] However, as shown in refs. [42,66], under standard operating conditions, there is no such difference between $R_{s,dark}$ and $R_{s,light}$.

Previously, the variation of the series resistance along the I–U curve was theoretically studied in detail by Araújo et al.,[46] and also they found a systematically lower $R_{s,dark}$ value. Note, however, that to include the dependence of the series resistance on the operating conditions, they modified the equivalent circuit by assuming a dependence of R_s on the strength of the external current. Using this approach, in a numerical study of a 1D model, they found a markedly different behavior of R_s in the short-circuit, nearly open-circuit, and the dark case. In contrast, using the Joule-loss-based definition for the series resistance for the same 1D model, we found no difference in the dark and the nearly open-circuit behavior, and we found a different short-circuit behavior that makes physically more sense.[42] We conclude that the results of Araújo et al. at least partly are artifacts due to their ad hoc modeling of the external current dependence of the series resistance.

To complete our considerations, we note that taking series-resistance effects into account in linear order helps to avoid the series-resistance averaging problem mentioned in Section 2 [cf. Equation (5)]. Applying a linear approximation to the exponential function in the local I–U characteristic, Equation (2), and using our LR-R_s series-resistance concept to describe the local voltage, Equation (3b), we arrive at

$$I_z(x,y) = I_{01}(x,y)\left[\left(1 - \frac{R_s(x,y)I_{ext}}{U_{th}}\right)\exp\left(\frac{U_{ext}}{U_{th}}\right) - 1\right] - I_{ph}(x,y) \tag{42}$$

In this approximation, we can write the lumped I–U characteristic, Equation (1), as

$$I_{ext} = I_{01}\left(1 - \frac{R_s I_{ext}}{U_{th}}\right)\exp\left(\frac{U_{ext}}{U_{th}}\right) - I_{01} - I_{ph} \tag{43}$$

while adding up the local I–U characteristics, Equation (42), we obtain

$$I_{ext} = \sum_{(x,y)} I_z(x,y) = \left[I_{01} - \left(\sum_{(x,y)} I_{01}(x,y)R_s(x,y)\right)\frac{I_{ext}}{U_{th}}\right] \times \exp\left(\frac{U_{ext}}{U_{th}}\right) - I_{01} - I_{ph} \tag{44}$$

In this expression, one can see a general feature relevant for series-resistance averaging: Local resistances contribute to the lumped behavior according to the current flowing through them. Now, for treating an inhomogeneous solar cell, we consider certain distributions for the local saturation currents and the local series resistances, expressing the local values by the deviations from the respective mean values of these distributions. Due to the arithmetic averaging rule that applies in our series-resistance modeling, Equation (22), these mean values are identical to the relevant lumped values

$$I_{01}(x,y) = \frac{1}{N}I_{01} + \Delta I_{01}(x,y),\ R_s(x,y) = R_s + \Delta R_s(x,y) \tag{45}$$

with the number N of local sites (x, y) considered. Using this in Equation (44), one has

$$I_{ext} = \left[I_{01} - \left(I_{01}R_s + \sum_{(x,y)} \Delta I_{01}(x,y)\Delta R_s(x,y)\right)\frac{I_{ext}}{U_{th}}\right] \times \exp\left(\frac{U_{ext}}{U_{th}}\right) - I_{01} - I_{ph} \tag{46}$$

as the sum of all deviations vanishes. For a solar cell that shows no cross-correlation between the distributions of series resistances and saturation currents, i.e., for which Equation (38) holds, also the remaining sum in Equation (46) vanishes, and we are left with the exact expression for the lumped I–U characteristic, Equation (43). As $\Delta R_s(x, y)$ is a smooth, laterally strongly correlated function, the cross-correlation will always vanish if the

© 2019 The Authors. Published by WILEY-VCH Verlag GmbH & Co. KGaA, Weinheim

$\Delta I_{01}(x, y)$ is randomly distributed. Therefore, a certain lateral clustering of $\Delta I_{01}(x, y)$ is needed to not fulfill Equation (43). Since clustering of defects is well known to induce lateral balancing currents across the 2D network of a solar cell, exactly the effects of lateral balancing currents are not included in the theory described in this work. Nevertheless, also lateral balancing currents can be easily dealt with in linear order in ρ_{sh} (cf. refs. [73,79]), but this is beyond the scope of the present work.

Finally, we note that not running into the inequality of Equation (5)—i.e., having instead that an equals sign holds in Equation (5)—does not imply that the standard equivalent circuit, Figure 1a, holds: It is possible to have equality in Equation (5) "pointwise" along the (lumped) *I–U* curve, however not with a constant global R_s (as in the standard equivalent circuit) but rather with different values of R_s for each dark current—which, as discussed earlier, turns out as a necessity to account for the distributed series resistance. To state it most clearly: Only with the modification introduced in the present work, the standard equivalent circuit may hold for a standard large-area silicon solar cell.

10. Conclusions

Due to the nonlinear diode characteristics and the distributed series-resistance network, some fundamental restrictions exist for averaging local solar-cell parameters; in general, the translation of local *I–U* curve parameters into lumped *I–U* curve parameters does not work. We have introduced and given reasons for a fundamental condition—that it is necessary and sufficient to consider distributed series-resistance effects in linear order in the sheet resistivity ρ_{sh}—which ensures that nearly all implicit expectations with respect to the applicability of the standard equivalent circuit for describing the lumped *I–U* curve of solar cells and the relation to local parameters hold. In the regime linear in ρ_{sh} and only in this order in ρ_{sh} it holds that 1) for local series resistance and local diode properties being spatially uncorrelated, the average voltage necessary to drive a total current through the local diodes is independent of ρ_{sh}, therefore averaging local diodes is independent of averaging local series resistances; 2) the average of the local diode resistances equals the lumped diode resistance; 3) for a given dark current, the arithmetic average of the local series resistances equals the lumped series resistance; 4) as a consequence of current redistribution between the emitter sheet and the p–n junction, occurring for increasing forward voltage, the average distributed series resistance is not constant but decreases for increasing dark diode forward current according to Equation (41); 5) the voltage varies linearly across the area of the solar cell; 6) no area loss occurs.

Experimentally, it was observed that the linear order in ρ_{sh} is the "natural" regime on standard industrial (i.e., "properly designed"/"economically reasonable") solar cells. We have obtained the relevant theoretical results by hierarchically solving the Helmholtz equation for the emitter voltage, obtained from the general differential equation by a linearization with respect to the diode conductivity, in different orders in the lateral resistivity. In contrast, a direct application of the general differential equation to a measured voltage distribution effectively means to look for a solution intrinsically nonlinear in ρ_{sh}. Thereby, however, the existing one—which is in linear order in ρ_{sh}—is hard to find; this also illustrates why the measurement noise has a drastic influence on Laplacian-based evaluation methods. The deeper physical reason behind is that the general differential equation incorporates the feedback of the voltage on the current distribution; however, no such feedback occurs on standard industrial ("properly designed"/"economically reasonable") solar cells.

On large-area silicon solar cells, the local junction current density determines the local Laplacian of the voltage, not the voltage itself; this is expressed by the general differential equation just mentioned. Therefore, the local voltage not only depends on the local junction current but also can be determined by all currents, especially the lateral ones. However, the conventional description of local series resistance, known as the model of independent diodes, links the local voltage to the local junction current only. This is in many ways unsuited for the description of large-area silicon solar cells. The conceptual starting point for the model of independent diodes is given by individually contacted, laterally fully isolated small solar-cell fragments. This accounts for all problems and contradictions occurring in the application of this model to large-area silicon solar cells: Lateral coupling effects between these fragments cannot be correctly accounted for, and the series resistance relevant for lateral balancing currents is significantly overestimated, especially for those running over short distances. The harmonic averaging procedure, inherent to the model of independent diodes, leads to another problem when this model is applied in a case where lateral currents dominate the voltage distribution and the influence of bulk resistances on the voltage distribution can be more or less neglected, as for vanishing sheet resistivity, $\rho_{sh} \to 0$, this averaging rule, $R_s^{-1} = N^{-1}\sum_{(x,y)} R_s^{-1}(x, y)$, breaks down: The terms diverge because all resistances go to zero. The usage of the model of independent diodes leads to various artifacts, e.g., in local series-resistance maps, most prominently in RESI images and known as "shunt paradox", or in current density maps, where they are termed "resistive blurring". Only in this model, it makes sense to plot an "open-circuit map" (providing a local U_{oc} value as if the whole solar cell behaved as this pixel); however, such a map contradicts the fundamental property of a strong coupling present in a 2D network due to lateral balancing currents which lead to the emitter nearly being an equipotential surface.

Experimentally, a meaningful value for the lumped series resistance—which depends on the chosen dark current—can always be obtained following the two-light-level method, and due to the dark-current dependence, this is the only meaningful way to define the lumped series resistance for large-area silicon solar cells. However, only in the case of a voltage distribution linear in ρ_{sh}, i.e., a voltage distribution linear across the area of the device, the lumped R_s value represents the Joule losses, and only then the equivalent circuit, modified to account for the dark-current dependence of R_s, may hold at all—and only then also a fit of the *I–U* curve to an expression resulting from the (modified!) equivalent circuit makes sense at all. As a consequence, any series-resistance measurement method also needs to use a fixed lumped dark current to provide physically meaningful values.

© 2019 The Authors. Published by WILEY-VCH Verlag GmbH & Co. KGaA, Weinheim

Altogether, our LR-R_s (linear-response series resistance) concept is based on the following principles: 1) For fixed lumped dark current, experiments show that emitter and grid of a properly designed/economically reasonable large-area silicon solar cell behave like a passive network and that lateral voltage variations show a proportionality to the current causing the voltage variations. The proportionality factor is defined as the relevant local series resistance. 2) The conceptual starting point for the description of the lateral voltage distribution for a large-area silicon solar cell at a fixed lumped dark current is the case of vanishing lateral series resistance; then, for all positions on the solar cell, the same potential holds (zeroth order approximation). The actual potential is obtained according to (1) as a deviation from the zeroth-order potential in linear order in the local series resistance and the total current. 3) Upon a variation of the lumped dark current, the lateral series resistance of a large-area silicon solar cell changes: The larger the dark current, the smaller the series resistance. This effect is fully contained in the newly proposed equivalent circuit, Figure 6.

In general, any local series-resistance concept that also provides a lumped R_s value must, by an appropriate averaging of the local values, deliver the value determined for the relevant dark current. In other words, if the average corresponding to a certain local series-resistance image/map does not equal the relevant lumped R_s value, this image/map does not represent the local series resistance.

As a practical consequence of the dark-current dependence of the series resistance, we mention that, unless an I–U measurement is corrected for the dark-current dependence of the series resistance, the latter may invalidate the interpretation of an observed injection dependence of other solar-cell properties derived from the I–U measurement. Moreover, even without injection-level dependence, the numerical values and the fit quality of standard I–U curve parameters can vary with the way the series resistance is treated.

As a concluding remark, we want to stress that the linear-response series-resistance concept introduced and discussed here needs as a starting point just the observation that there are large-area silicon solar cells which are able to deliver the photocurrent from their whole area without any current losses. This implies that emitter and grid of such a solar cell introduce series-resistance effects in linear order in the sheet resistivity—and in linear order only; this further implies that the standard equivalent circuit model holds for such a solar cell. In this work, we show how easy a theory for the full description of all relevant local and lumped series-resistance effects can be for such solar cells. Physicists and materials scientists should benefit from this knowledge for a deeper understanding of series-resistance networks and their (local or lumped) characterization. If higher-order sheet-resistivity effects have to be considered, the concept of splitting up the solar-cell network into a (lumped) diode and a (lumped) series resistance (i.e., using the standard equivalent circuit) does not simplify the description anymore.

Supporting Information

Supporting Information is available from the Wiley Online Library or from the author.

Acknowledgements

J.-M.W. acknowledges financial support from the Chair of Functional Nanomaterials, Technical Faculty, University of Kiel, as well as the support and encouragement of Prof. H. Föll.

Conflict of Interest

The authors declare no conflict of interest.

Keywords

equivalent circuit, Joule losses, local series resistance, solar cell modeling, voltage losses

Received: July 21, 2019
Revised: September 26, 2019
Published online: December 22, 2019

[1] T. Trupke, E. Pink, R. A. Bardos, M. D. Abbott, *Appl. Phys. Lett.* **2007**, *90*, 093506.
[2] D. Hinken, K. Ramspeck, K. Bothe, B. Fischer, R. Brendel, *Appl. Phys. Lett.* **2007**, *91*, 182104.
[3] J. Carstensen, A. Schütt, H. Föll, in *Proc. 22nd European Photovoltaic Solar Energy Conference*, WIP, Munich **2007**, contribution 1CV.1.34.
[4] K. Ramspeck, K. Bothe, D. Hinken, B. Fischer, J. Schmidt, R. Brendel, *Appl. Phys. Lett.* **2007**, *90*, 153502.
[5] B. Michl, M. Kasemann, J. Giesecke, M. Glatthaar, A. Schütt, J. Carstensen, H. Föll, S. Rein, W. Warta, H. Nagel, in *Proc. 23rd European Photovoltaic Solar Energy Conference*, WIP, Munich **2008**, contribution 2DO.2.5.
[6] H. Kampwerth, T. Trupke, J. W. Weber, Y. Augarten, *Appl. Phys. Lett.* **2008**, *93*, 202102.
[7] J. Haunschild, M. Glatthaar, M. Kasemann, S. Rein, E. R. Weber, *Phys. Status Solidi RRL* **2009**, *3*, 227.
[8] O. Breitenstein, A. Khanna, Y. Augarten, J. Bauer, J.-M. Wagner, K. Iwig, *Phys. Status Solidi RRL* **2010**, *4*, 7.
[9] M. Glatthaar, J. Haunschild, M. Kasemann, J. Giesecke, W. Warta, S. Rein, *Phys. Status Solidi RRL* **2010**, *4*, 13.
[10] M. Glatthaar, J. Haunschild, R. Zeidler, M. Demant, J. Greulich, B. Michl, W. Warta, S. Rein, R. Preu, *J. Appl. Phys.* **2010**, *108*, 014501.
[11] J.-M. Wagner, J. Carstensen, A. Berhane, A. Schütt, H. Föll, in *Proc. 26th European Photovoltaic Solar Energy Conference*, WIP, Munich **2011**, contribution 2BV.2.51.
[12] J. Wong, *IEEE Trans. Electron Devices* **2013**, *60*, 917.
[13] C. Shen, H. Kampwerth, M. Green, T. Trupke, J. Carstensen, A. Schütt, *Sol. Energy Mater. Sol. Cells* **2013**, *109*, 77.
[14] C. Shen, M. Green, O. Breitenstein, T. Trupke, M. Zhang, H. Kampwerth, *Sol. Energy Mater. Sol. Cells* **2014**, *123*, 41.
[15] O. Breitenstein, H. Hoffler, J. Haunschild, *Sol. Energy Mater. Sol. Cells* **2014**, *128*, 296.
[16] O. Breitenstein, J. Bauer, D. Hinken, K. Bothe, *Sol. Energy Mater. Sol. Cells* **2015**, *137*, 50.
[17] O. Breitenstein, *Sol. Energy Mater. Sol. Cells* **2011**, *95*, 2933.
[18] J. Liu, A. Melnikov, A. Mandelis, *Phys. Status Solidi A* **2013**, *210*, 2135.
[19] O. Breitenstein, J. Bauer, D. Hinken, K. Bothe, *Sol. Energy Mater. Sol. Cells* **2015**, *142*, 92.
[20] F. Frühauf, O. Breitenstein, *Sol. Energy Mater. Sol. Cells* **2016**, *146*, 87.
[21] O. Breitenstein, J. P. Rakotoniaina, M. H. Al Rifai, *Prog. Photovoltaics* **2003**, *11*, 515.

© 2019 The Authors. Published by WILEY-VCH Verlag GmbH & Co. KGaA, Weinheim

[22] M. Kasemann, M. C. Schubert, M. The, M. Köber, M. Hermle, W. Warta, *Appl. Phys. Lett.* **2006**, *89*, 224102.
[23] Y. Augarten, M. D. Abbott, T. Trupke, R. Bardos, H. P. Hartmann, R. Gupta, J. Bauer, O. Breitenstein, in *Proc. 22nd European Photovoltaic Solar Energy Conference*, WIP, Munich **2007**, contribution 2CV.3.49.
[24] M. Kasemann, D. Grote, B. Walter, W. Kwapil, T. Trupke, Y. Augarten, R. A. Bardos, E. Pink, M. D. Abbott, W. Warta, *Prog. Photovoltaics* **2009**, *16*, 297.
[25] Y. Augarten, T. Trupke, M. Lenio, J. Bauer, O. Breitenstein, J. Weber, R. A. Bardos, in *Proc. 24th European Photovoltaic Solar Energy Conference*, WIP, Munich **2009**, contribution 1AO.4.2.
[26] Y. Augarten, T. Trupke, M. Lenio, J. Bauer, J. W. Weber, M. Juhl, M. Kasemann, O. Breitenstein, *Prog. Photovoltaics* **2013**, *21*, 933.
[27] O. Breitenstein, *Sol. Energy Mater. Sol. Cells* **2012**, *107*, 381.
[28] A. Mandelis, Y. Zhang, A. Melnikov, *J. Appl. Phys.* **2012**, *112*, 054505.
[29] O. Breitenstein, J. Carstensen, A. Schütt, J.-M. Wagner, in *Proc. 28th European Photovoltaic Solar Energy Conference*, WIP, Munich **2013**, contribution 2CV.3.15.
[30] O. Breitenstein, C. Shen, H. Kampwerth, M. A. Green, *Energy Procedia* **2013**, *38*, 2.
[31] F. Fertig, J. Greulich, S. Rein, *Appl. Phys. Lett.* **2014**, *104*, 201111.
[32] F. Fertig, J. Greulich, S. Rein, *J. Appl. Phys.* **2014**, *116*, 184501.
[33] O. Breitenstein, F. Fertig, J. Bauer, *Sol. Energy Mater. Sol. Cells* **2015**, *143*, 406.
[34] J. Wong, M. A. Green, *Phys. Rev. B* **2012**, *85*, 235205.
[35] J. Wong, R. Sridharan, Y. C. Wang, T. Mueller, in *Proc. 40th IEEE Photovoltaic Specialists Conference*, IEEE, New York/Piscataway **2014**, p. 975.
[36] U. Rau, V. Huhn, L. Stoicescu, M. Schneemann, Y. Augarten, A. Gerber, B. E. Pieters, *Appl. Phys. Lett.* **2014**, *105*, 163507.
[37] M. Wolf, H. Rauschenbach, *Adv. Energy Convers.* **1963**, *3*, 455.
[38] D. K. Bhattacharya, A. Mansingh, P. Swarup, *Sol. Cells* **1986**, *18*, 153.
[39] P. P. Altermatt, G. Heiser, A. G. Aberle, A. Wang, J. Zhao, S. J. Robinson, S. Bowden, M. A. Green, *Prog. Photovoltaics* **1996**, *4*, 399.
[40] S. Bowden, A. Rohatgi, in *Proc. 17th European Photovoltaic Solar Energy Conference*, WIP, Munich **2001**, 1802.
[41] K. C. Fong, K. R. McIntosh, A. W. Blakers, *Prog. Photovoltaics* **2013**, *21*, 490.
[42] J.-M. Wagner, A. Schütt, J. Carstensen, R. Adelung, *Energy Procedia* **2016**, *92*, 255.
[43] K. Rajkanan, J. Shewchun, *Solid-State Electron.* **1979**, *22*, 193.
[44] G. M. Smirnov, J. E. Mahan, *Solid-State Electron.* **1980**, *23*, 1055.
[45] S. R. Dhariwal, S. Mittal, R. K. Mathur, *Solid-State Electron.* **1984**, *27*, 267.
[46] G. L. Araújo, A. Cuevas, J. M. Ruiz, *IEEE Trans. Electron Devices* **1986**, *33*, 391.
[47] A. Vishnoi, R. Gopal, R. Dwivedi, S. K. Srivastava, *IEE Proc.-G: Circuits, Devices, Systems* **1993**, *140*, 155.
[48] S. Sokolic, D. Krizaj, S. Amon, *Solid-State Electron.* **1993**, *36*, 623.
[49] J. L. Boone, T. P. van Doren, *IEEE Trans. Electron Devices* **1978**, *25*, 767.
[50] L. D. Nielsen, *IEEE Trans. Electron Devices* **1982**, *29*, 821.
[51] M. Bashahu, A. Habyarimana, *Renew. Energy* **1995**, *6*, 129.
[52] D. Pysch, A. Mette, S. W. Glunz, *Sol. Energy Mater. Sol. Cells* **2007**, *91*, 1698.
[53] D. T. Cotfas, P. A. Cotfas, S. Kaplanis, *Renew. Sustain. Energy Rev.* **2013**, *28*, 588.
[54] K. Bothe, D. Hinken, in *Semiconductors and Semimetals*, Vol. *89* (Eds: G. P. Willeke, E. R. Weber), Academic Press, Cambridge, MA **2013**, p. 259.
[55] G. M. M. W. Bissels, J. J. Schermer, M. A. H. Asselbergs, E. J. Haverkamp, P. Mulder, G. J. Bauhuis, E. Vlieg, *Sol. Energy Mater. Sol. Cells* **2014**, *130*, 605.
[56] G. Micard, G. Hahn, in *Proc. 28th European Photovoltaic Solar Energy Conference*, WIP, Munich **2013**, contribution 2BO.2.5.
[57] A. S. H. van der Heide, J. Poortmans, in *Proc. 35th European Photovoltaic Solar Energy Conference*, WIP, Munich **2018**, contribution 2DV.3.13.
[58] J. Carstensen, J.-M. Wagner, A. Schütt, H. Föll, in *Proc. 29th European Photovoltaic Solar Energy Conference*, WIP, Munich **2014**, contribution 2BV.8.21.
[59] P. E. Mijnarends, G. J. M. Janssen, W. C. Sinke, *Sol. Energy Mater. Sol. Cells* **1994**, *33*, 345.
[60] J.-M. Wagner, M. Hoppe, A. Schütt, J. Carstensen, H. Föll, *Energy Procedia* **2013**, *38*, 199.
[61] U. Rau, P. O. Grabitz, J. H. Werner, *Appl. Phys. Lett.* **2004**, *85*, 6010.
[62] P. O. Grabitz, U. Rau, J. H. Werner, *Phys. Status Solidi A* **2005**, *202*, 2920.
[63] O. Breitenstein, S. Rißland, *Sol. Energy Mater. Sol. Cells* **2013**, *110*, 77.
[64] H. Höffler, H. Al-Mohtaseb, J. Haunschild, B. Michl, M. Kasemann, *J. Appl. Phys.* **2014**, *115*, 034508.
[65] H. Höffler, H. Al-Mohtaseb, N. Wöhrle, B. Michl, M. Kasemann, J. Haunschild, *Energy Procedia* **2014**, *55*, 85.
[66] J.-M. Wagner, K. Upadhyayula, J. Carstensen, R. Adelung, *AIP Conf. Proc.* **2018**, *1999*, 020022.
[67] J. Carstensen, A. Abdollahinia, A. Schütt, H. Föll, in *Proc. 24th European Photovoltaic Solar Energy Conference*, WIP, Munich **2009**, contribution 1CV.4.33.
[68] J.-M. Wagner, K. Upadhyayula, J. Carstensen, R. Adelung, *AIP Conf. Proc.* **2019**, *2147*, 020019.
[69] J. Carstensen, A. Schütt, H. Föll, in *Proc. 23rd European Photovoltaic Solar Energy Conference*, WIP, Munich **2008**, contribution 1CV.1.38.
[70] M. Glatthaar, J. Giesecke, M. Kasemann, J. Haunschild, M. The, W. Warta, S. Rein, *J. Appl. Phys.* **2009**, *105*, 113110.
[71] N. Convers Wyeth, *Solid-State Electron.* **1977**, *20*, 629.
[72] A. G. Aberle, S. R. Wenham, M. A. Green, in *Proc. 23rd IEEE Photovoltaic Specialists Conference*, IEEE, New York/Piscataway **1993**, p. 133.
[73] J. Carstensen, J.-M. Wagner, A. Schütt, A. Krudopp, H. Föll, in *Proc. 29th European Photovoltaic Solar Energy Conference*, WIP, Munich **2014**, contribution 2BO.2.6.
[74] M. Turek, *J. Appl. Phys.* **2014**, *115*, 144503.
[75] J. Granlund, *IEEE Electron Device Lett.* **1980**, *1*, 151.
[76] G. L. Araújo, A. Cuevas, J. M. Ruiz, in *Proc. 6th European Photovoltaic Solar Energy Conference*, D. Reidel Publishing Co., Dordrecht **1985**, p. 138.
[77] J.-M. Wagner, S. Rißland, A. Schütt, J. Carstensen, R. Adelung, *Energy Procedia* **2017**, *124*, 197.
[78] R. M. Swanson, R. A. Sinton, in *Advances in Solar Energy*, Vol. *6* (Ed: K. W. Böer), Plenum Press, New York **1990**, p. 427.
[79] J. Carstensen, J.-M. Wagner, A. Schütt, R. Adelung, in *Proc. 31st European Photovoltaic Solar Energy Conference*, WIP, Munich **2015**, contribution 2BV.8.22.
[80] G. N. Watson, *A Treatise on the Theory of Bessel Functions*, Cambridge University Press, Cambridge, UK **1944**.

© 2019 The Authors. Published by WILEY-VCH Verlag GmbH & Co. KGaA, Weinheim